Transactions of the Korean Nuclear Society Spring Meeting
Jeju, Korea, May 23-24, 2019

Electrochemical Roles of Lead Species on Stress Corrosion Cracking of Alloy 600

Do Haeng Hur*, Won-Ik Choi, Geon Dong Song, Soon-Hyeok Jeon
Nuclear Materials Research Division, Korea Atomic Energy Research Institute,
989-111, Daedeok-daero, Yuseong-gu, Daejeon, 34057, Republic of Korea
**Corresponding author: dhhur@kaeri.re.kr*

1. Introduction

Lead (Pb) has been known to accelerate stress corrosion cracking (PbSCC) of Alloy 600, 690, and 800 in various simulated secondary environments of steam generators in pressurized water reactors. The important experimental results on PbSCC can be summarized as follows: PbSCC is the most aggressive in alkaline solutions [1,2]; Pb-species are detected in oxide films and inside cracks [3,4]; Cracks are filled with corrosion products [3,4]; Crack path is changed from an intergranular mode in grain boundary chromium carbide-free microstructures to a transgranular mode in grain boundary carbide-decorated ones [5,6].

However, most experimental studies have reported only a change of phenomenon with the addition of Pb-species. In addition, most of the test solutions were too unrealistically strong to appropriately simulate the crevice conditions encountered in operating SGs. Furthermore, the electrochemical role of Pb has not been systemically addressed so far. SCC occurs basically via an electrochemical process under the simultaneous aid of tensile stress. Therefore, elucidating the role of Pb-species for how to alter the oxide property and how to affect the cracking process is crucial to understand the mechanism of PbSCC. Therefore, this work focuses on the electrochemical roles of Pb-species during the processes of oxide formation, growth, and crack advance of Alloy 600 in simulated secondary water with and without 100 ppm PbO at 315 °C.

2. Experimental

All specimens were prepared from Alloy 600 sheets, which were annealed at 1060 °C for 2.5 min, followed by water quenching.

Electrochemical polarization tests were performed in simulated secondary water with and without 100 wt. ppm PbO at 280 °C, whose pH was adjusted to 9.0 at 25°C using NaOH. After the open-circuit potential (OCP) reached a steady value at 280°C, polarization measurements were conducted from the OCP toward the cathodic or the anodic direction at a scan rate of 30 mV/min. Individual anodic and cathodic polarization curve were finally combined into a graph.

SCC tests were conducted at 315 °C using U-bend specimens in the same solutions as those used in the electrochemical tests. For the tests in the PbO-free solution, the autoclave operation was stopped to examine the U-bend specimens after the first 650 h and every 500 h subsequently until the test time reached 5,000 h in total. The test solution was refreshed and deaerated whenever the autoclave was closed after inspection of the test specimens. On the other hand, the duration of testing in the PbO-containing solution was 350 h and 650 h, respectively, because cracks were observed even after 350 h.

After the SCC tests, the U-bend specimens were destructively examined to measure the depth and morphology of the cracks. Oxides on the surfaces and inside cracks were also analyzed by using TEM-EDS and XPS.

3. Results

Fig. 1 shows the polarization curves of Alloy 600 in the test solutions with and without 100 ppm PbO at 280°C. The corrosion potential was approximately 160 mV higher in the PbO-solution than the PbO-free solution. The overall anodic current density of Alloy 600 also increased in the PbO-solution.

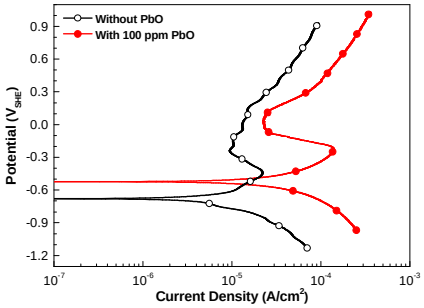

Fig. 1. Effect of lead oxide on the polarization behaviors of Alloy 600 in the test solutions at 280 °C.

As shown in Fig. 2, no cracks were observed in the U-bend specimens up to an exposure of 5,000 h to the PbO-free solution. However, many cracks were observed in the 100 ppm PbO solution even after 350 h. The maximum crack depth on average was 186 μm after 350 h and 326 μm after 650 h.

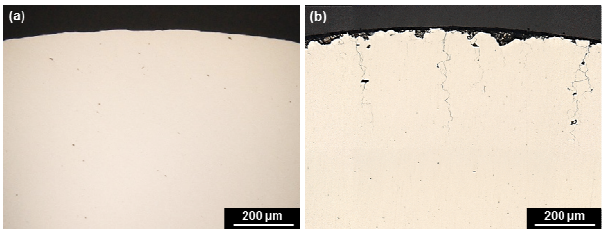

Fig. 2. Cross-sections of the U-bend specimens after the SCC tests: (a) in the PbO-free solution after 5000 h, (b) in the 100 ppm PbO solution after 650 h.

Fig. 3 shows the SEM images on the outer surfaces of the U-bend specimens. The grinding marks were apparent in the PbO-free solution, but they were completely covered with oxides in the PbO solution. This result indicates that PbO significantly accelerated corrosion from the alloy matrix.

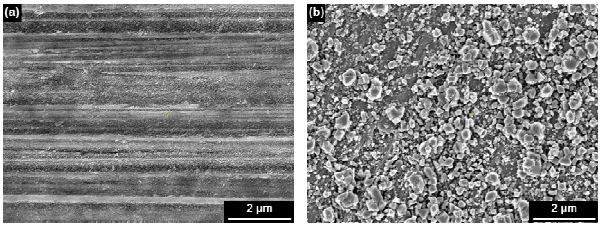

Fig. 3. SEM images on the outer surfaces of the U-bend specimens after the SCC tests: (a) in the PbO-free solution after 650 h and (b) in the 100 ppm PbO solution after 650 h.

This phenomenon is again demonstrated in Fig. 4(a) and (c), showing the cross-sectional scanning TEM (STEM) images of the oxide layers near the apex region of the U-bend specimens. The thickness was increased by approximately 2.4 times with the addition of 100 ppm PbO. From Fig. 4(b), the outermost oxide layer formed in the PbO-free solution was too extremely thin to distinguish the interface between the outermost oxide and inner oxide. Cr was significantly enriched in the outermost oxide layer and then gradually decreased toward the matrix, resulting in Ni depletion. As shown in Fig. 4(d), the large oxide particles formed in the PbO solution were nearly pure Ni-oxides (NiO) containing minor Fe. The inner oxide beneath these particles was also enriched in Cr and depleted in Ni. However, the Cr content of the inner oxide in the PbO solution was roughly half of that of the oxide in the PbO-free solution. Notably, Pb was significantly concentrated in the outermost layer of the inner oxide and thereafter gradually decreased.

In order to determine the chemical states of the detected Pb-species, XPS analysis was performed on the surface oxide and on the fracture surface of a crack grown in the PbO solution for 650 h. As shown in Fig. 5, the peaks of $Pb(OH)_2$ and PbO decreased with the sputtering time, whereas the peak of the metallic lead (Pb^0) gradually increased simultaneously. Thus, the fraction of the metallic Pb was increased from the surface to the alloy matrix.

4. Discussion

Figs. 1~4 indicate that the corrosion rate including the dissolution and oxidation of the alloy matrix was accelerated by the addition of PbO. In addition, Cr dissolution from the matrix was accelerated by the addition of PbO, resulting in the oxide formation with a relatively lower Cr content (Fig. 4). Therefore, this compositional change in the inner oxide can become a cause of the fast cracking in the PbO solution.

The XPS results demonstrate an enrichment of metallic Pb toward the matrix. From the potential–pH diagrams of the Pb–H_2O system at 300°C [1,7,8], the thermodynamically stable form of Pb in the test solution at 315 ℃ is $Pb(OH)^+$ or $Pb(OH)_2$(aq.). These soluble Pb-species can migrate from the bulk solution to the alloy surface and they can be electrochemically reduced on the surface through the following reactions. Here, the thermodynamic calculation was performed using the HSC Chemistry 6 software [9].

$$Pb(OH)^+ + H^+ + Ni \rightarrow Pb + Ni^{2+} + H_2O \quad (\Delta G_{315°C} = -69\ kJ/mol) \quad (1)$$

$$Pb(OH)^+ + H^+ + Cr \rightarrow Pb + Cr^{2+} + H_2O \quad (\Delta G_{315°C} = -200\ kJ/mol) \quad (2)$$

$$Pb(OH)^+ + H^+ + Fe \rightarrow Pb + Fe^{2+} + H_2O \quad (\Delta G_{315°C} = -124\ kJ/mol) \quad (3)$$

$$Pb(OH)_2(aq.) + 2H^+ + Ni \rightarrow Pb + Ni^{2+} + 2H_2O \quad (\Delta G_{315°C} = -204\ kJ/mol) \quad (4)$$

$$Pb(OH)_2(aq.) + 2H^+ + Cr \rightarrow Pb + Cr^{2+} + 2H_2O \quad (\Delta G_{315°C} = -335\ kJ/mol) \quad (5)$$

$$Pb(OH)_2(aq.) + 2H^+ + Fe \rightarrow Pb + Fe^{2+} + 2H_2O \quad (\Delta G_{315°C} = -259\ kJ/mol) \quad (6)$$

The above reactions are all thermodynamically possible. Consequently, the soluble Pb-species can be electrochemically reduced to metallic Pb, which in return increases the dissolution of the alloy elements from the matrix in the PbO solution.

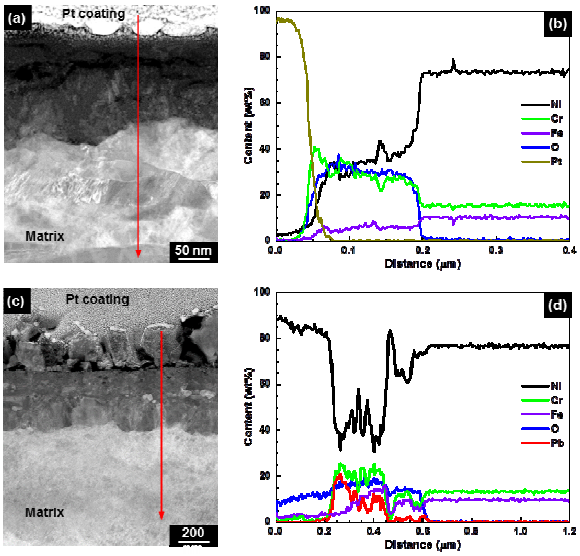

Fig. 4. STEM images on the outer surfaces of the U-bend specimens after the SCC tests: (a) in the PbO-free solution after 650 h and (b) in the 100 ppm PbO solution after 650 h.

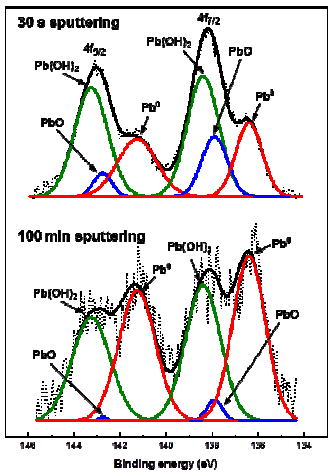

Fig. 5. XPS spectra of Pb obtained on the surface oxides formed in the 100 ppm PbO solution after 650 h.

The accelerated dissolution of the alloy elements from the matrix by the reduction of Pb-species inevitably increases lattice vacancies and their clusters, which in turn provide paths to facilitate the migration of Pb-species from the bulk solution to the interface between the inner oxide and matrix. As shown in Fig. 4(d), a high Pb content was still detected even at the inner oxide/matrix interface. This strongly demonstrates that defective oxides are formed, which facilitate the penetration of Pb-species through the oxide layer.

The soluble Pb-species can also be electrochemically reduced through the following reactions:

$$Pb(OH)^+ + Ni \rightarrow Pb + NiO + H^+ \quad (\Delta G_{315°C} = -32\ kJ/mol) \quad (7)$$

$$3Pb(OH)^+ + 2Cr \rightarrow 3Pb + Cr_2O_3 + 3H^+ \quad (\Delta G_{315°C} = -519\ kJ/mol) \quad (8)$$

$$4Pb(OH)^+ + 3Fe \rightarrow 4Pb + Fe_3O_4 + 4H^+ \quad (\Delta G_{315°C} = -306\ kJ/mol) \quad (9)$$

Therefore, the above spontaneous reactions indicate that the reduction of Pb-species can induce the oxide formation of the alloy elements. Thus, the much thicker oxides observed in the PbO solution can be attributed to these reactions. Finally, it can be concluded that the increased corrosion rate including dissolution and oxidation in the PbO solution is explained by the electrochemical reduction of Pb-species through reactions (1)-(9). Therefore, these reactions demonstrate the following results obtained in the PbO solution: the increased polarization current in Fig. 1, the thick oxide formation in Figs. 3-4, and the detected metallic Pb in Fig. 5.

5. Conclusions

Based on the experimental observations and thermodynamic considerations, the mechanistic model for fast cracking of Alloy 600 by lead contamination can be described sequentially as follows: Pb-species are electrochemically reduced to metallic Pb on the surface, leading to an accelerated dissolution of the alloy elements (preferentially Cr) from the matrix and oxidation of the matrix. Defects such as vacancy clusters or nanovoids, which can be formed through the accelerated dissolution of the alloy elements, provide paths for the migration of Pb-species toward the matrix. The electrochemical reactions for the reduction of Pb-species and the corresponding dissolution and oxidation of the matrix continue to occur at the oxide/matrix interface, resulting in the formation of thick and defective films with a relatively lower Cr. These oxide films lead to the fast initiation of SCC under a tensile stress. Once a micro-crack is initiated, the aforementioned process occurs repeatedly on the exposed bare surface inside the crack.

Acknowledgement

This work was supported by the National Research Foundation of Korea (NRF) grant funded by the Korea government (NRF-2017M2A8A4015159).

REFERENCES

[1] EPRI, Investigation of Lead as a Cause of Stress Corrosion Cracking at Support Plate Intersections, EPRI, Palo Alto, USA (1991) NP-7367-S.
[2] R.W. Staehle, “Assessment of and proposal for a mechanistic interpretation of the SCC of high nickel alloys in lead containing environments”, Proceedings of the 11th International Conference on Environmental Degradation of Materials in Nuclear Power Systems – Water Reactors, (2003) 381-424.
[3] B.T. Lu, J.L. Luo, Y.C. Lu, J. Electrochem. Soc. 154 (2007) C379-C389.
[4] S.M. Bruemmer and L.E. Thomas, Surf. Interface Anal. 31 (2001) 571-581.
[5] G.P. Airey, The effect of carbon content and thermal treatment on the SCC behavior of Inconel Alloy 600 steam generator tubing, Corrosion 35 (1979) 129-136.
[6] J.M. Sarver, “IGSCC of nickel alloys in lead contaminated high purity water”, EPRI Workshop in Intergranular Corrosion and Primary Water Stress Corrosion Cracking Mechanisms, EPRI-NP-5971, EPRI, Palo Alto, CA, USA (1987) C11/1.
[7] R.W. Staehle, “Clues and issues in the SCC of high nickel alloys associated dissolved lead”, Proceedings of the 12th International Conference on Environmental Degradation of Materials in Nuclear Power Systems – Water Reactors, TMS, (2005) 1163-1209.
[8] E. Protopopoff and P. Marcus, J. Electrochem. Soc. 164 (2017) C164-C170.
[9] HSC Chemistry 6, version 6.12, Outotec Research Oy, Pori, Filand.